Optical distinction and photoinduced phase transition between degenerate ground states of polyacene

ARTICLE *in* PHYSICA B CONDENSED MATTER · JUNE 2010

Impact Factor: 1.32 · DOI: 10.1016/j.physb.2009.11.106

2 AUTHORS, INCLUDING:

Shoji Yamamoto
Hokkaido University
124 PUBLICATIONS **1,881** CITATIONS

Physica B 405 (2010) S365–S368

Contents lists available at ScienceDirect

Physica B

journal homepage: www.elsevier.com/locate/physb

Optical distinction and photoinduced phase transition between degenerate ground states of polyacene

Shoji Yamamoto [a,*], Jun Ohara [b]

[a] Department of Physics, Hokkaido University, Sapporo 060-0810, Japan
[b] Division of Physics, Yokohama National University, Yokohama 240-8501, Japan

ARTICLE INFO

Keywords:
Polyacene
Peierls instability
Optical conductivity
Photoinduced phase transition

ABSTRACT

We investigate the ground-state properties of polyacene in terms of an extended Peierls-Hubbard Hamiltonian with particular emphasis on its structural instability of two types: double bonds in a *cis* pattern and those in a *trans* pattern. The two Peierls-distorted states are degenerate in their energetics but quite distinct in their optics. The *trans* configuration is easily photoconverted into the *cis* one, whereas an opposite transition, if any, is hardly completed. Domain-wall (soliton) excitations play an important role in any photoinduced phase transitions, but charged and neutral ones behave quite differently.

Although polyacene is the simple polymer next to polyacetylene, its electronic structure is still controversial. In contrast with the Peierls instability in polyacetylene [1], polyacene suffers from structural instability only conditionally [2]. Therefore, a numerous effort [3] has been devoted to clarifying whether and how the Peierls distortion occurs in polyacene. Under competing electron-electron and electron-lattice interactions, both uniform and distorted structures can appear in the ground state (cf. Fig. 1), the former of which may be either aromatic or antiferromagnetic, while the latter of which are further classified into *cis* and *trans* configurations.

Early investigations focused on predicting which of them should be the ground state, but their consequences varied with the computational method. Quality *ab initio* calculations [4] showed the aromatic configuration to be slightly favored over any distorted structure, while a variety of semiempirical molecular-orbital calculations [5–8] concluded the Kekulé structures to be energetically preferable, where both *cis* and *trans* configurations were nominated for the most stable, however. In recent years sophisticated numerical tools [9–11] have revealed that the *cis* distortion is lower in energy than the *trans* one. Such a controversy strongly suggests that uniform and Peierls-distorted states should closely compete with each other in any case and may coexist due to local defects and/or thermal excitations in actual polyacene.

In such circumstances, there may not be much meaning in energetically ranking these low-energy states in more detail. We should instead take an interest in any other features in an attempt at identifying and possibly controlling the ground state of polyacene. Thus motivated, we discuss optical properties of polyacene with particular emphasis on the two structural isomers of distinct bond alternation. We describe polyacene in terms of an extended Peierls-Hubbard Hamiltonian:

$$\begin{aligned}\mathcal{H}=&-\sum_{l=1}^{2}\sum_{n=1}^{N}\sum_{s=\pm}[(t_{\parallel}-\alpha r_{l:2n-1})c^{\dagger}_{l:2n-1,s}c_{l:2n,s}+(t_{\parallel}-\alpha r_{l:2n})c^{\dagger}_{l:2n,s}c_{l:2n+1,s}\\&+\mathrm{H.c.}]-t_{\perp}\sum_{n=1}^{N}\sum_{s=\pm}(c^{\dagger}_{1:2n-1,s}c_{2:2n-1,s}+\mathrm{H.c.})+\frac{K}{2}\sum_{l=1}^{2}\sum_{n=1}^{N}(r^{2}_{l:2n-1}\\&+r^{2}_{l:2n})+U\sum_{l=1}^{2}\sum_{n=1}^{N}\left[\left(n_{l:2n-1,+}-\frac{1}{2}\right)\left(n_{l:2n-1,-}-\frac{1}{2}\right)\right.\\&\left.+\left(n_{l:2n,+}-\frac{1}{2}\right)\left(n_{l:2n,-}-\frac{1}{2}\right)\right]\\&+V_{\parallel}\sum_{l=1}^{2}\sum_{n=1}^{N}\sum_{s,s'=\pm}\left(n_{l:2n,s}-\frac{1}{2}\right)(n_{l:2n-1,s'}+n_{l:2n+1,s'}-1)\\&+V_{\perp}\sum_{n=1}^{N}\sum_{s,s'=\pm}\left(n_{1:2n-1,s}-\frac{1}{2}\right)\left(n_{2:2n-1,s'}-\frac{1}{2}\right),\end{aligned}\tag{1}$$

where $c^{\dagger}_{l:j,s}$ and $c_{l:j,s}$ ($c^{\dagger}_{l:j,s}c_{l:j,s}\equiv n_{l:j,s}$) create and annihilate, respectively, a π electron of spin s at site j on chain l, while $r_{l:j}$ denotes the bond distortion caused by the j th and $(j+1)$ th carbon atoms on the l th chain. The Coulomb interactions, ranging over neighboring sites, are modeled in $V_{\parallel(\perp)}=U/\kappa\sqrt{1+0.6117a^{2}_{\parallel(\perp)}}$ [12], where κ is a dielectric parameter, while $a_{\parallel}$ and $a_{\perp}$ are the average lengths in Å of neighboring C–C leg and rung bonds, respectively. We adopt the screened Coulomb parametrization,

* Corresponding author. Tel.: +81 11 706 2681; fax: +81 11 706 2681.
E-mail address: yamamoto@phys.sci.hokudai.ac.jp (S. Yamamoto).

0921-4526/$ - see front matter © 2009 Elsevier B.V. All rights reserved.
doi:10.1016/j.physb.2009.11.106

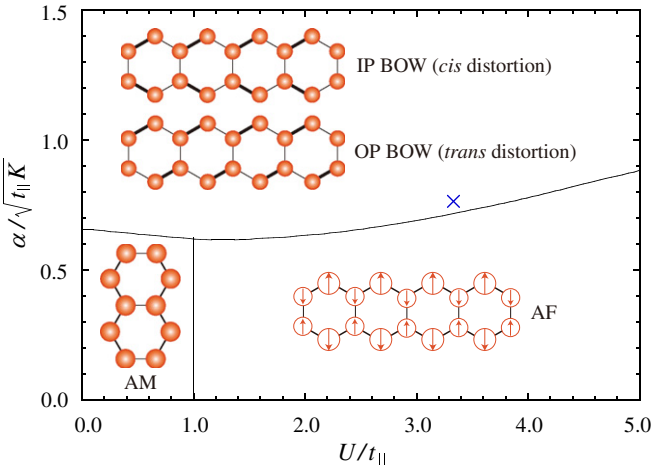

Fig. 1. HF calculation of a ground-state phase diagram on the α-U plain at $N=64$. $\times$ denotes the present parametrization.

$U=8.0\,\mathrm{eV}$ and $\kappa=2.0$ [13], with $a_{\parallel}=1.4\,\text{Å}$ and $a_{\perp}=1.5\,\text{Å}$ [14]. The intrachain and interchain hopping energies are taken as $t_{\parallel}=2.4\,\mathrm{eV}$ [13] and $t_{\perp}=0.864t_{\parallel}$ [15]. Fig. 1 demonstrates various phases competing in the ground state. We find a metallic state of aromatic (AM) configuration, an antiferromagnetic (AF) Mott insulator, and *cis*- and *trans*- distorted Peierls insulators, which are here referred to as in-phase (IP) and out-of-phase (OP) bond-order-wave (BOW) states, respectively. There is no energy difference between IP and OP BOWs within the Hartree–Fock (HF) scheme. They are so degenerate as to have the same energy even in more sophisticated calculations such as modified-neglect-of-diatomic-overlap [8] and many-body valence-bond [16] descriptions of Kekulé structures. Since we take a particular interest in the two Peierls-distorted isomers, we adopt the electron-lattice coupling constant $\alpha=4.1\,\mathrm{eV/Å}$ together with the σ- bond elastic constant $K=12.0\,\mathrm{eV/Å}^2$.

Fig. 2(a) shows the HF single-particle energy spectra of IP and OP BOWs. Every molecular orbital can be characterized as either

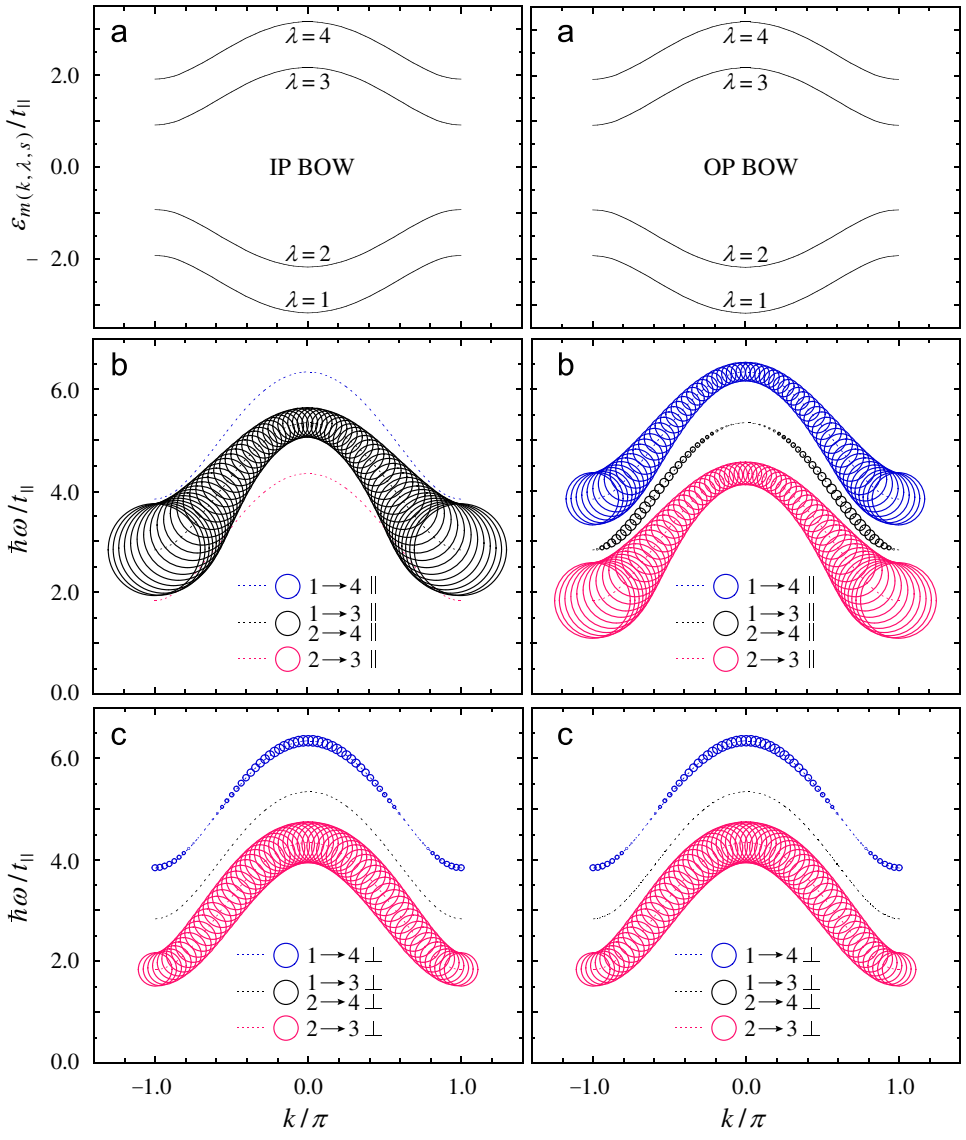

Fig. 2. HF calculations of the dispersion relations of the π- electron valence ($\lambda=1,2$) and conduction ($\lambda=3,4$) bands (a) and the "momentum (k)-resolved" polarized optical conductivity parallel (b) and perpendicular (c) to the long axis for IP BOW and OP BOW at $N=64$, where the area of each circle corresponds to the spectral weight.

symmetric or antisymmetric with respect to reflection about the plane bisecting every rung bond. Symmetric ones constitute the bands of $\lambda=1$ and 3, while antisymmetric ones assemble into those of $\lambda=2$ and 4. IP and OP BOWs share such an energetics [10], though they possess distinct properties of global symmetry operation [7,17]: the former is C_2- and σ_v- invariant, whereas the latter is C_2'- invariant.

Then we are led to investigate their optics. The real part of the optical conductivity reads [18]

$$\sigma_{\parallel,\perp}(\omega)=\frac{\pi}{\omega}\sum_l |\langle E_l|\mathcal{J}_{\parallel,\perp}|E_0\rangle|^2\delta(E_l-E_0-\hbar\omega), \quad (2)$$

where $\mathcal{J}_\parallel$ and $\mathcal{J}_\perp$ are the current operators along the long and short axes, respectively, while $|E_l\rangle$ denotes a wave vector of the l th-lying state of energy E_l. Since any transition of finite momentum transfer is optically forbidden, a HF excited state and its energy read $|E_{l(k,\mu,\nu,s)}\rangle_{\rm HF}=a^\dagger_{m(k,\nu,s)}a_{m(k,\mu,s)}|E_0\rangle_{\rm HF}$ and $E_{l(k,\mu,\nu,s)}={}_{\rm HF}\langle E_0|\mathcal{H}|E_0\rangle_{\rm HF}-\varepsilon_{m(k,\mu,s)}+\varepsilon_{m(k,\nu,s)}$, respectively, provided $\mu=1,2$ and $\nu=3,4$, where $|E_0\rangle_{\rm HF}\equiv\prod_{m=1}^{4N}a_m^\dagger|0\rangle$ is the HF ground-state wave function with $|0\rangle$ being the true electron vacuum and $a_m^\dagger$ creating an electron in the m th HF orbital of energy ε_m. We plot the spectral weight $(\pi/\omega)\sum_s|\langle E_l|\mathcal{J}|E_0\rangle|^2\delta(E_l-E_0-\hbar\omega)$ as a function of k and (μ,ν) in Figs. 2(b) and (c). 1-to-3 and 2-to-4 excitations are equivalent in every aspect because of the electron-hole symmetry. IP and OP BOWs remain exhibiting the same optical features as long as the excitation light is polarized in the rung direction, where all the 1-to-3 and 2-to-4 excitations, with parity unchanged, are optically forbidden. On the other hand, photoirradiation in the leg direction reveals a striking contrast between IP and OP BOWs.

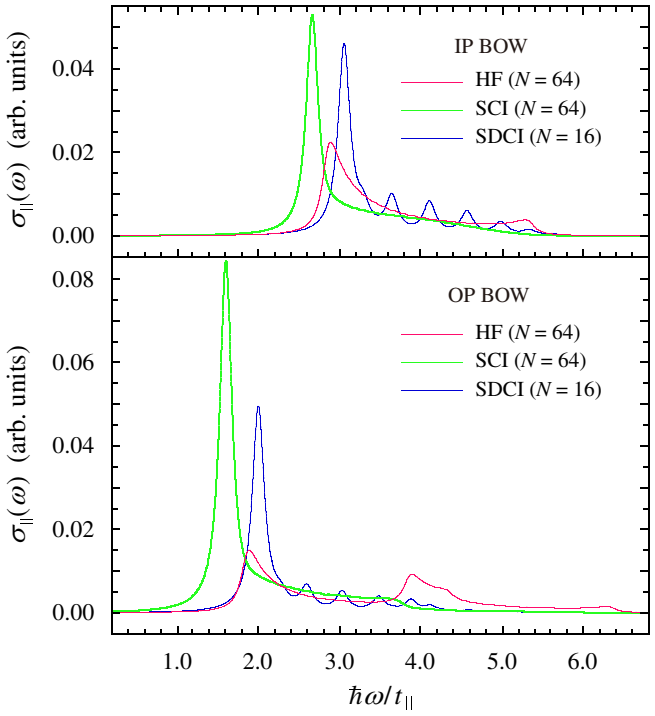

Fig. 3. HF, SCI, and SDCI calculations of the long-axis-polarized optical conductivity spectrum for IP and OP BOWs at $N=64$. Every spectral line is Lorentzian broadened by a width of $0.09t_\parallel$.

The thus-characterized dipole transition matrices are summed up and corrected under many-body effects in Fig. 3. State vectors of the configuration-interaction (CI) type consist of resonating Slater determinants [11]. Exited-state Slater determinants of the double-excitation type are much more important than those of the single-excitation type, because only they can directly interact with the HF wave function. IP and OP BOWs are quite distinct in their optics. The highest-occupied-molecular-orbital (HOMO)-to-lowest-unoccupied-molecular-orbital (LUMO) transition through a long-axis-polarized photon is allowed in OP BOW but forbidden in IP BOW. Judging from the most reliable single-double-excitation CI (SDCI) findings, the HF approximation overestimates high-energy 1-to-4 transition matrices but reproduces the optical gap much better than the single-excitation CI (SCI) scheme. Thus convinced, we next simulate the system photoexcited employing a time-dependent HF method [19].

We photoinduce low-energy electron-hole pairs, that is to say, 2-to-3 excitations at $k\simeq\pm\pi$. Fig. 4 visualizes lattice dynamics of the thus-excited OP-BOW state. We have calculated initial conditions of every kind under low light intensity but observed only local collapse of the OP-BOW structure irradiated within three photons (per 64 benzene rings). When the light intensity is so increased that a photon is found every 16 benzene rings, the OP-BOW structure is globally converted into the IP-BOW one, which is detectable with the other order parameter $R_j^{(+)}=(-1)^j(r_{1;j}+r_{2;j})/2$. Such a nonlinearity is widely observed in photoinduced phase transitions [20,21]. However, whether and how the phase transition is accomplished depend on the initial nucleation inevitably stochastic. Charge excitations without any spin fluctuations [Fig. 4(c)] are apt to form charged solitons,

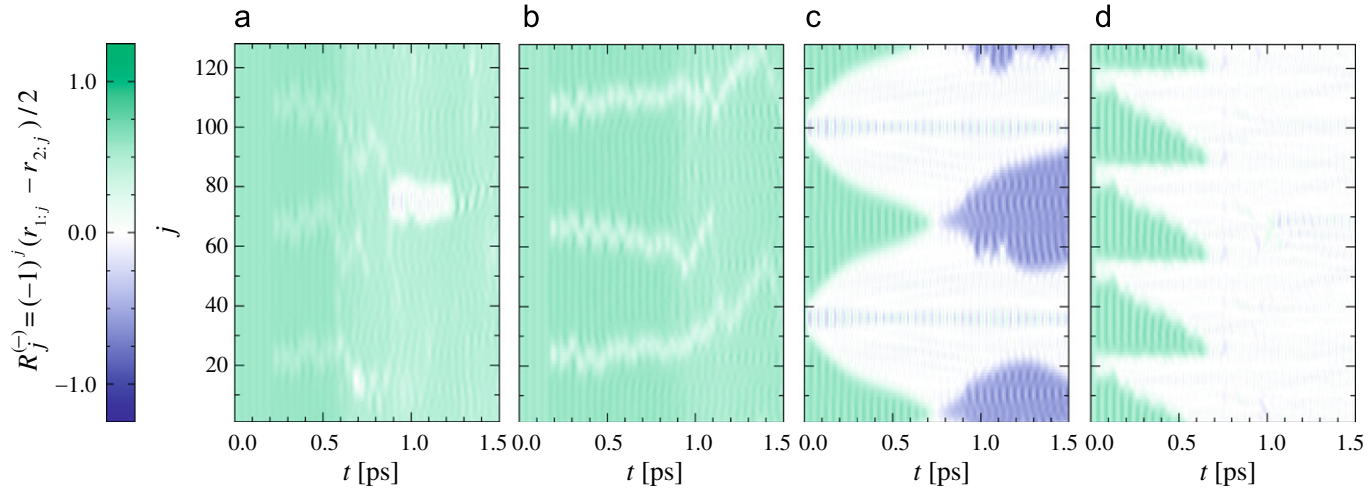

Fig. 4. Contour plots of an OP-BOW-detectable bond variable on the OP-BOW background as functions of space and time. At $t=0$ we excite one electron (a), two electrons (b), four electrons without any spin fluctuations (c), and four electrons with local spin fluctuations (d) from the HOMO(s) to the LUMO(s).

where positively and negatively charged ones are separated into two chains and are therefore long-lived. Consequently the OP-BOW structure is broken but recovered. There are different ways of exciting two or more electrons. Photoexcited two unpaired up- and down-spin electrons [Fig. 4(d)], together with two more electrons in a singlet pair, grow into neutral solitons and they are all localized onto one leg of the ladder. Those with opposite spins soon come across each other and suffer geminate recombinations. The IP-BOW structure thus settles down. In contrast to OP-to-IP BOW transitions, IP-to-OP ones, if any, often end incompletely. The IP-BOW structure looks much more persistent against photoirradiation. Further investigations, as well as graphic analyses in more detail, will be reported elsewhere.

References

[1] H.C. Longuet-Higgins, L. Salem, Proc. Roy. Soc. A 251 (1959) 172.
[2] L. Salem, H.C. Longuet-Higgins, Proc. Roy. Soc. A 255 (1960) 435.
[3] M. Bendikov, F. Wudl, D.F. Perepichka, Chem. Rev. 104 (2004) 4891.
[4] J. Cioslowski, J. Chem. Phys. 98 (1993) 473.
[5] M.-H. Whangbo, R. Hoffmann, R.B. Woodward, Proc. Roy. Soc. A 366 (1979) 23.
[6] K. Tanaka, K. Ohzeki, S. Nankai, T. Yamabe, H. Shirakawa, J. Phys. Chem. Solids 44 (1983) 1069.
[7] M. Kertesz, Y.S. Lee, J.J.P. Stewart, Int. J. Mod. Chem. 35 (1989) 305.
[8] J. Chandrasekhar, P.K. Das, J. Phys. Chem. 96 (1992) 679.
[9] B. Srinivasan, S. Ramasesha, Phys. Rev. B 57 (1998) 8927.
[10] C. Raghu, Y. Anusooya Pati, S. Ramasesha, Phys. Rev. B 65 (2002) 155204.
[11] S. Yamamoto, Phys. Rev. B 78 (2008) 235205.
[12] K. Ohno, Theor. Chim. Acta 2 (1964) 219.
[13] P. Sony, A. Shukla, Phys. Rev. B 75 (2007) 155208.
[14] M. Bendikov, H.M. Duong, K. Starkey, K.N. Houk, E.A. Carter, F. Wudl, J. Am. Chem. Soc. 126 (2004) 7416.
[15] Z. An, C.Q. Wu, Eur. Phys. J. B 42 (2004) 467.
[16] M.A. Garcia-Bach, A. Peñaranda, D.J. Klein, Phys. Rev. B 45 (1992) 10891.
[17] K. Funase, S. Yamamoto, J. Phys. Soc. Japan 75 (2006) 044717.
[18] S. Yamamoto, J. Ohara, Phys. Rev. B 76 (2007) 235116.
[19] S. Yamamoto, J. Ohara, J. Phys. Condens. Matter 20 (2008) 415215.
[20] K. Iwano, Phys. Rev. B 61 (2000) 279.
[21] K. Yonemitsu, N. Miyashita, Phys. Rev. B 68 (2003) 075113.